Applied Surface Science 306 (2014) 27–32

Contents lists available at ScienceDirect

Applied Surface Science

journal homepage: www.elsevier.com/locate/apsusc

MOCVD selective growth of orthorhombic or hexagonal $YMnO_3$ phase on Si(1 0 0) substrate

I. Iliescu*, M. Boudard, L. Rapenne, O. Chaix-Pluchery, H. Roussel

Laboratoire des Matériaux et du Génie Physique, UMR 5628 CNRS-Grenoble INP, Minatec, 3 parvis Louis Néel, CS 50257, 38016 Grenoble Cedex 1, France

ARTICLE INFO

Article history:
Received 25 October 2013
Received in revised form 11 January 2014
Accepted 15 January 2014
Available online 25 January 2014

Keywords:
$YMnO_3$ film on silicon substrate
MOCVD
Multiferroics

ABSTRACT

Multiferroic $YMnO_3$ (YMO) thin films were grown by pulsed injection metal organic chemical vapor deposition on (1 0 0)-oriented silicon substrate. The growth conditions were optimized in order to obtain either orthorhombic (o-YMO) or hexagonal (h-YMO) YMO phases. The most significant deposition parameters in the selective growth of these phases are the substrate temperature and the Y/Mn ratio in the precursor solution. Polycrystalline films with a preferential growth direction are obtained for h-YMO whereas grains with random orientation are observed for o-YMO as shown by X-ray diffraction and transmission electron microscopy. The h-YMO (300 nm thick) and o-YMO (450 nm thick) films present a columnar growth with column diameter comprised between 15 and 35 nm. The Raman spectrum of o-YMO film is reported and compared to the o-YMO bulk spectrum. The temperature-dependent magnetization curves display a λ-shape for both o- and h-YMO phases, indicating a spin-glass state.

1. Introduction

Multiferroic materials, in which more than one ferroic order coexist, have received much attention in the last decades because of their potential in applications such as spintronics, data storage, sensors, actuators and ferroelectric technology. The most representative multiferroics are usually perovskite-type oxides, which are very interesting from a fundamental point of view due to the strong electronic correlations present in these systems. Among these oxides, $YMnO_3$ (YMO) has been intensively studied in order to fully understand its crystal structure and multiferroic properties. As bulk material, it presents two crystal structures with different Bravais lattices: hexagonal, corresponding to a thermodynamically stable phase (h-YMO), and orthorhombic, corresponding to a metastable form (o-YMO). The o-YMO can be stabilized under high pressure conditions [1], using soft chemistry methods [2], or grown as thin films thanks to epitaxial stabilization by clamping on a perovskite-type substrate [3]. Its structure (space group *Pnma*, $a = 5.8361(2)$ Å, $b = 7.3571(3)$ Å, $c = 5.2580(2)$ Å [4]) consists of basic polyhedral units built up by Mn^{3+} ions at the center of MnO_6 octahedra. These units are interconnected by sharing their vertices along three perpendicular directions and Y^{3+} ions occupy the holes between them. The structure of the h-YMO phase (space group $P6_3cm$, $a = 6.1453(2)$ Å and $c = 11.3714(5)$ Å [5]) consists of two non-connected layers of MnO_5 trigonal bipyramid, separated by a layer of Y^{3+} ions. The Mn^{3+} ions have 5-fold coordination and are located at the center of the MnO_5 trigonal bipyramid. These basic MnO_5 units build a layer by interconnection of their vertices to form a triangular tiling. The structural differences for o-YMO and h-YMO lead to different physical properties. The h-YMO phase shows an antiferromagnetic order below the Néel temperature $T_N \sim 73$ K [6] and a ferroelectric order below Curie temperature $T_C \sim 910$ K [7] while the o-YMO phase presents an antiferromagnetic order below $T_N \sim 42$ K [2] and a ferroelectric order below $T_C \sim 35$–40 K [8].

In relation with technological applications, Fujimura et al. have proposed the potential use of thin films of h-YMO, grown by rf magnetron sputtering, as non-volatile memory devices [9]. Since then, an extensive work was carried out on YMO films grown from several techniques: pulsed laser deposition [3], rf sputtering [10], metal organic chemical vapor deposition (MOCVD) [11], chemical solution deposition [12], sol gel [13], molecular beam epitaxy [14] or atomic layer deposition [15]. As far as YMO film on Si substrate is concerned, these previous works report mainly h-YMO as the major phase and only scarce results are presented for o-YMO phase [16,17].

In the present work, films of either h-YMO or o-YMO phase were selectively grown by pulsed injection MOCVD. The structural properties and morphologies of both films are studied in detail and compared.

* Corresponding author. Tel.: +33 04 56 52 93 28.
E-mail address: ionela.iliescu@grenoble-inp.fr (I. Iliescu).

http://dx.doi.org/10.1016/j.apsusc.2014.01.090
0169-4332/

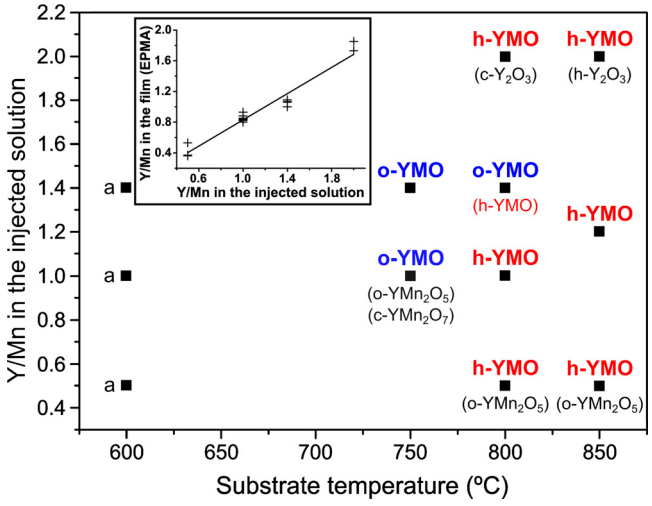

Fig. 1. Experimental phase diagram of YMO film as a function of the Y/Mn atomic ratio in the injected solution and substrate temperature ("a" denotes the amorphous phase). Secondary phases are designated in parentheses. An almost linear trend between the Y/Mn ratio in the injected solution and the Y/Mn ratio in the film, measured by EPMA technique, is shown in the inset (dispersion in the data is mainly due to different deposition temperatures and thermal stabilities of precursors).

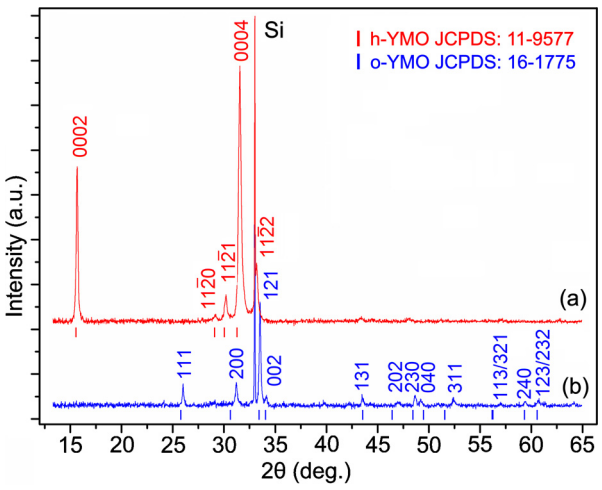

Fig. 2. XRD patterns of YMO films obtained by selective growth using MOCVD: (a) h-YMO film; (b) o-YMO film. All reflections are indexed with h-YMO (a) or o-YMO (b) phase. The position of the reflections for bulk h-YMO (o-YMO) phase according to the JCPDS cards are indicated in the figure by vertical red lines (vertical blue lines). Si denotes the Si substrate. The XRD pattern in (a) indicates that the h-YMO film is textured. The XRD pattern in (b) indicates that the o-YMO is a randomly oriented polycrystalline film. (For interpretation of the references to color in this figure legend, the reader is referred to the web version of the article.)

2. Experimental details

YMO films were deposited on (1 0 0)-oriented silicon substrate (Si(1 0 0)) using a pulsed injection MOCVD type reactor previously described in [18]. The crystal structure of the films was investigated by X-ray diffraction (XRD), in θ–2θ geometry using a monochromatic Cu$K_{\alpha 1}$ radiation (λ = 1.5406 Å) with a Bruker D8 Advance diffractometer. Detailed structural characterizations of the films were carried out by transmission electron microscopy (TEM) observations using a JEOL 2010 microscope operating at 200 kV with a beam current of 110 mA (0.19 nm resolution). For cross-section imaging, the samples were prepared by mechanical polishing (tripode technique) perpendicular to the film surface using diamond lapping films to achieve sample thickness close to 10 μm. The final thinning was performed by the precision ion polishing system (with milling angle ±7° at 3.2 KeV) in order to obtain large electron transparent area. The surface morphology and thickness of the films were analyzed using a field emission gun type scanning electron microscope (FEI QUANTA 250 ESEM FEG). The overall atomic compositions and the film thicknesses were determined by electron probe micro analysis (EPMA) using a CAMECA SX50 spectrometer. Raman spectra were recorded at room temperature with a Horiba/Jobin Yvon LabRam spectrometer. The 514.5 nm Ar^+ laser line was used for excitation. Typical Raman spectra were obtained for an acquisition time varying between 400 and 900 s. The magnetic measurements of the YMO samples were carried out with a SQUID MPMS magnetometer from Quantum Design. The temperature dependence of the magnetization ($M(T)$) curves in zero-field-cooled (*ZFC*) and field-cooled (*FC*) mode was studied in the 4–300 K temperature range with an applied in-plane field of 500 Oe. The magnetization curves as a function of the magnetic field ($M(H)$) measurements were recorded between −50 and +50 kOe at 5 and 300 K.

3. Results and discussion

Either the h-YMO or the o-YMO phase was selectively grown by varying mainly the Y/Mn atomic ratio in the injected solution and the substrate temperature used in the MOCVD as shown in Fig. 1. Whereas in the low temperature range (600 °C) all the as-deposited YMO films were amorphous whatever the composition used in the injected solution, at higher temperatures (750–850 °C) it is possible to obtain either the h-YMO or the o-YMO phase by the optimal tuning of the MOCVD parameters. In particular, Fig. 1 shows that the h-YMO phase can be obtained when the deposition takes places at 800 °C using an Y/Mn atomic ratio in the injected solution of 1. Alternatively, the o-YMO phase can be obtained when samples are deposited at 750 °C with an Y/Mn atomic ratio in the injected solution of 1.4. The optimal deposition parameters appear to represent a relative sharp window and small departures lead to secondary Y-rich or Mn-rich phases (see Fig. 1). It is worth noting that the present work is the first report on the stabilization of the metastable o-YMO phase deposited on Si(1 0 0) substrate, without using any epitaxial strain mechanism. In the following, a detailed structural analysis will be presented for two films deposited with the optimized MOCVD parameters presented above: T = 800 °C, Y/Mn = 1 for the hexagonal phase; T = 750 °C, Y/Mn = 1.4 for the orthorhombic phase (hereafter h-YMO and o-YMO will refer to these films).

The XRD patterns of h-YMO and o-YMO films are shown in Fig. 2. They clearly indicate that the h-YMO (Fig. 2(a)) or the o-YMO (Fig. 2(b)) phases are present, as far as XRD is concerned, but the presence of amorphous or nanocrystalline phases cannot be ruled out (see next paragraphs concerning TEM results). They also indicate that whereas the h-YMO film is strongly *c*-axis textured, i.e. most of the grains grow with the (0 0 0 *l*) planes parallel to the Si surface (see assignment of the intense diffraction lines in the figure), the o-YMO film grows on the Si substrate without any particular orientation, having the characteristics of a polycrystalline powder.

The lattice parameters for the h-YMO film determined from the XRD pattern (a = 6.129(3) Å, c = 11.354(3) Å) are in good agreement with the data in JCPDS card No. 11-9577 (a = 6.1453 Å, c = 11.3714 Å) corresponding to the stoichiometric h-YMO phase [5]. This is an indication that our samples are close to the stoichiometric values, but spreading of the data in the literature avoid further comparison (e.g. $YMnO_3$: a = 6.138(4), c = 11.407(3) [6]; a = 6.1542(3), c = 11.4031(2) [19]; $YMnO_{2.91}$: a = 6.137(9), c = 11.411(2) [6]; $YMnO_{2.95}$: a = 6.1728(2), c = 11.4509(4) [19]; $YMnO_{2.85}$: a = 6.1806(1), c = 11.4545(4) [19]).

The lattice parameters obtained from the XRD pattern for o-YMO film in Pnma setting (a = 5.734(3) Å, b = 7.381(3) Å, c = 5.258(3) Å)